Adapting rainfed rice to climate change: a case study in Senegal

Edward Gérardeaux, Gatien Falconnier, Eric Gozé, Dimitri Defrance, Paul-Martial Kouakou, Romain Loison, Benjamin Sultan, François Affholder, Bertrand Muller

Agronomy for Sustainable Development (2021) 41: 57
https://doi.org/10.1007/s13593-021-00710-2

RESEARCH ARTICLE

Adapting rainfed rice to climate change: a case study in Senegal

Edward Gérardeaux[1,2] · Gatien Falconnier[1] · Eric Gozé[1] · Dimitri Defrance[9] · Paul-Martial Kouakou[4] · Romain Loison[2,5,6] · Benjamin Sultan[3] · François Affholder[1] · Bertrand Muller[7,8]

Accepted: 14 June 2021 / Published online: 2 August 2021

Abstract

Rainfed crop production predominates in West Africa. Rice is an important staple food, especially in Senegal. The scope for increase in rice production under irrigated conditions is uncertain. Rainfed rice is therefore a key component for regional food security impelling agronomists to assess climate change impact on rainfed rice yield and to design rainfed rice ideotypes suited to future climate scenarios. The DSSAT CSM-CERES-Rice model was thus calibrated and evaluated on 19 agronomic experiments conducted in 2012, 2013, and 2014, in 6 locations, with 21 cultivars and two fertilization levels (20 and 80 kg N ha^{-1}). Simulations were then carried out with the crop model forced with the downscaled projections of seven climate models, with and without considering the impact of an increase in atmospheric [CO_2], using an ensemble of global circulation models and two Representative Concentration Pathways (RCP2.6 and RCP8.5). Simulated rice yield was divided by two over the century with RCP8.5 and stagnated with RCP2.6. Elevated [CO_2] significantly increased yields, but this effect could not offset the yield decline due to elevated temperatures. Cultivars with longer vegetative phases and greater temperature tolerance were better adapted to climate change than current cultivars. Using these new cultivars with the recommended fertilization rate (80 kg N ha^{-1}) could offset the yield decline due to climate change. For the first time, we bring together a study based on a process-based crop model handling crop response to elevated [CO_2], a large set of field experiments and up-to-date climate projections (i) to provide useful insights into plausible impacts of climate change on rainfed rice in Senegal and (ii) to identify cultivar characteristics relevant for adaptation to future possible climates. Our findings will help set priorities for breeding resilient cultivar in the region.

Keywords *Oryza sativa* · Crop modeling · Cultivar · Ideotype · CSM-CERES-Rice · Carbon dioxide

1 Introduction

Rice is the world's most important food crop, estimated as the staple food for half of humanity. The demand for rice is expected to increase with population growth. West African countries like Senegal, Guinea-Bissau, and Guinea are highly dependent on rice for food calories. According to the International Food Policy Research Institute (Glatzel 2018), the average Senegalese consumes about 85 kg of rice each year. The government has embarked on political efforts to achieve self-sufficiency for rice, with public investments, price protection, and extension services reinforcement. The national long-term economic development strategy targets rice self-sufficiency for the country by 2035. The efforts focus on both irrigated and rainfed rice. After a marked decline during the dry decades at the end of the previous century, rainfed rice cultivation has expanded rapidly in Senegal, especially in Kaffrine, Senegal oriental, and Casamance regions. In the above-mentioned regions, the rainy season covers only 5 months, from June to October. Despite the strong political

✉ Edward Gérardeaux
gerardeaux@cirad.fr

1 CIRAD, UPR AIDA, F-34398 Montpellier, France
2 AIDA, Univ Montpellier, CIRAD, Montpellier, France
3 ESPACE-DEV, Univ Montpellier, IRD, Univ Guyane, Univ Réunion, Univ Antilles, Univ Avignon, Maison de la Télédétection, 500 rue Jean-François Breton, F-34093 Montpellier, France
4 INP-HB Yamassoukro, Yamassoukro, Côte d'Ivoire
5 CIRAD, UPR AIDA, Dakar, Senegal
6 SODEFITEX, Dakar, Senegal
7 CIRAD, UMR AGAP, F-34398 Montpellier, France
8 Univ Montpellier, CIRAD, Montpellier, France
9 The Climate Data Factory, 12 rue de Belzunce, 75010 Paris, France

commitment to improve rice production, inadequate water, soil, and crop management still compromises paddy yield productivity. Rice production is also threatened by variability in annual rainfall, fluctuations in the onset of growing season, and increase in aridity (Koudahe et al. 2017). Assessments of the changes in local climatic variables and their impact on rice yield are currently scarce.

Water availability for crops in Africa varies strongly over space and time. It is a major constraint for the continent's economic development, which may become even stronger with climate warming. In most regions of sub-Saharan Africa, climate change will likely increase water stress with detrimental effects on crop yield (Roudier et al. 2011). Ensuring sustainable agriculture in semi-arid to sub-humid Africa requires adaptation to climatic variability and change.

Climate change, as simulated by Global Climate Models (GCM), includes a gradual increase in temperature, modification of rainfall patterns and amounts, and increase in the frequency of extreme events (Barry et al. 2018). The impacts of these perturbations on rice cropping systems in Asia have been extensively investigated (Li et al. 2015; Kontgis et al. 2019). Impact studies on rainfed rice in Sudanian regions of Africa are much scarcer, despite the fact that rice is one of the major staple food. Global assessments, including the whole Africa, have been performed, but they are not based on model calibration with accurate field data (Oort and Zwart 2017). In West Africa, an increase in the frequency and the magnitude of extreme events (heavy rains, heat waves) is expected as well as a decline and a slight increase in annual rainfall in the west and east of the region, respectively (Diedhiou et al. 2018). Rainfed crop production dominates in West Africa, making the region a climate change hotspot. To our knowledge, among the very few studies focusing on the impact of climate change on rice yield in West Africa (Zhang et al. 2019; Traore et al. 2020), none used a process-based crop model, calibrated and evaluated for a set of cultivars based on field measurements. These studies based on statistical modelling overlooked the impact of elevated [CO_2] on crop growth.

Breeding cultivars with adequate characteristics can offset yield losses by limiting rice sterility with high temperatures (Jagadish et al. 2015). Adequate characteristics identified with field and glasshouse experiments include increased transpiration cooling, early morning flowering, shifts in phenology to avoid stresses, and increased spikelet numbers and sink strength (Sheehy et al. 2001). Experiments on specific physiological capacities and omics investigations of a large number of traits and their interactions require resources and take time. Plant traits expression and its impact on yield also vary with agronomic practices. Increasing the amount of applied mineral fertilizer can improve crop yield. However, rainfed cropping systems prevail in Senegal and drought can severely undermine the benefits related to mineral fertilizer application. Unfavorable value/cost ratio currently prevent adoption of increased rates of mineral fertilizer application (Jayne et al. 2018). Crop simulation models can integrate the knowledge on physiological processes to help explain yield limitations in varying environments and agrosystems. CSM-CERES-Rice has been used in India and China for investigating climate change impacts on rice production (Yao et al. 2007). With calibrated cultivar parameters used as proxy for physiological traits, the model can help investigate genotype*environment interactions and design rice ideotypes for adaptation to climate change as it was done for other crops and models (Rötter et al. 2015).

In this study, we examined the potential impact of climate change on rainfed rice yield in Senegal. We based our assessment on the calibration of a crop model on a large field trials dataset with 21 different cultivars and multiple environments. Simulations were carried-out with a crop model that took as daily input the downscaled projections of seven climate models to take into account the uncertainties in climate projections. We also simulated possible adaptations strategies using ideotypes with adaptive traits.

2 Material and methods

In order to provide useful predictions, a model has to be calibrated locally. To search for ideotypes, this has to be done on a set of contrasted cultivars, of which we expect that the parameters genotypic variability will reflect the cultivated diversity.

2.1 Environments

Nineteen field trials were carried out from 2012 to 2014 in the Sudanian and Sudano-Sahelian zones of Senegal to test the adaptation of rice cropping systems to drought conditions. Six sites (see fig. 1 in supplementary materials) were considered: Darou (13° 57′36″ N/15° 50′24″ W), Sinthiou Maleme (13° 49′48″ N/13° 54′36″ W), Ndama (13° 49′12″ N/15° 4 2′01″ W), Diéri (13° 37′12″ N/15° 34′12″ W), Kolda (12° 51′36″ N/14° 57′00″ W), and Sefa (12°49′48″ N/15° 35′24″ W). Current average rainfall from June to October is 500–600 mm, 600–700 mm, 600–700 mm, 700–800 mm, 900–1000 mm, and 1000–1100 mm in the different sites, respectively. The experimental sites were chosen to cover the range of pedoclimatic conditions found in South and East Senegal (Fig. 1), where rainfed rice is one of the main crops. Diéri and Ndama hosted farmers field experiments, while the other sites hosted on-station controlled experiments.

The experimental design at all sites was fully randomized blocks with three to four replicated plots, two fertilization rates, and 4 to 21 cultivars tested in each experiment. Plot size was 2.5 m wide × 3 m long = 7.5 m^2, with 10 rows and 15 hills

Fig. 1 Rainfed rice cultivar experiments in Senegal 2012. Left: An agronomical trial set in ISRA Sinthiou Malème research station (on sandy soil). Right: A rainfed farmer field near Kolda. (photograph by B. Muller).

per row. The dataset was divided into a calibration and a validation dataset (Table 1). Each cultivar was grown under two fertilization rates, namely F1=80 kg N ha^{-1} and F2=20 kg N ha^{-1}, either in controlled conditions or on farmers' fields. Observation on on-station plots (averaged across replicates) with F1=80 kg N ha^{-1} (assumed to be stress-free conditions) were used for model calibration. On-station plots with F2=20 kg N ha^{-1} and plots in farmers' field experiments were used for model validation (Table 1).

2.2 Weather data

Daily rainfall data was collected on experimental sites with rain gauges. Daily temperatures were collected on sites with automatic sensors Tinytag Plus 2 (Tinytag) placed under shelter (in Sefa, Darou, Kolda) or at the closest official meteorological station (Nioro station 13°45′00″N/15°48′00″ W) for Dieri Kao and Ndama sites. Relative humidity and global radiation were collected at the closest station of the public network of meteorological stations, at Kolda (12° 53′00″ N/14° 57′00″ W) for Kolda and Sefa and at Nioro for Dieri Kao, Ndama, and Darou. All Sinthiou data were collected on site through an automatic agrometeorological station CIMEL ENERCO 405 (© Cimel Electronique S.A.S France). The data was collected from 2012 to 2014.

2.3 Cultivars

The 21 cultivars used in the experiment were either hybrids, japonica, or indica type and came from various breeding centers (Table 2).

2.4 Soil sampling and analysis

Agricultural soils in Senegal are well known, and many of their chemical and physical properties in deeper layers can be relatively well derived from key properties of the top layers using reference soil profiles. Soil analyses were conducted on four soil samples per experiment, done at 3 depths (0–10, 10–20, and 20–30 cm) and averaged. Soil depth in the region is also known to be either over 5m, i.e., much greater than rooting depth of most annual crops, or very shallow when soils are on lateritic deposits. In each experimental location, auger prospection down to 1 m deep was carried out to ensure that soils belong to the former case. Physical and chemical properties were analyzed at ISRA laboratory at Bambey. All soils were sandy, i.e., none of them had more than 20 % clay + silt (Table 1). Carbon, organic matter, and organic nitrogen contents were low, and pH in water ranged from 5.3 to 7.2.

2.5 Plant observations

Rice anthesis and maturity were observed on the main stem of six plants per plots. Anthesis and maturity dates corresponded to the date when three plants out of the six had reached the stage. Biomass at anthesis was measured on 10 hills randomly taken on two side lines.

Grain weight, plant biomass, number of spikelets, tillers, and grains were measured at harvest on a central subplot (6 lines × 7 hills). All plants samples were dried at 65 ° during 72 h before weighing.

2.6 Simulation of rice growth

The DSSAT 4.7.1.0 cropping system model (DSSAT-CSM) (Boote et al. 2003) was used. DSSAT-CSM simulates soil nitrogen, water, and carbon dynamics. CSM-CERES-Rice

Table 1 Year, site, crop management, soil properties, and rainfall distribution in the experiments in Senegal used for DSSAT calibration and validation. *das* days after sowing, *Fert* fertilizer treatment, with F1: recommended dose (80 kg N ha^{-1}), i.e., 200 kg ha^{-1} NPK (15.15.15) at sowing + 100 kg ha^{-1} urea at 20 das + 50 kg ha^{-1} urea at 50 das. F2: F1/4 (20 kg N ha^{-1}); *C/V/P* calibration/validation/projection. *C/V* calibration on F1 and validation on F2; cultivars 1 to 21, DJ11, DK17, DK2, DK3, FK45, INTA, IR10, ITA, NE1, NE11, NE12, NE14, NE17, NE4, NE6, NE8, NE9, W181, W189, W5650, WC165; in the soil properties, *C* carbon, *OM* organic matter, *N* nitrogen.

Year	Site	Use	Cultural practices																						Soil properties (0–30 cm)							Rainfall (mm)	
			Cultivars																						Sowing date	Fert.	Plant density (nb m^{-2})	Clay+ Silt (%)	C (‰)	OM (‰)	Organic N (‰)	pH water	0–60 das	60–90 das
			1	2	3	4	5	6	7	8	9	10	11	12	13	14	15	16	17	18	19	20	21											
2012	Darou	C/V	x	x	x	x			x	x	x	x	x	x	x	x	x	x	x	x	x	x		20/07	F1/F2	44	9.8	3.1	5.3	0.13	7.2	546	144
2012	Kolda	C/V	x	x	x	x			x	x	x	x	x	x	x	x	x	x	x	x	x	x		21/07	F1/F2	59	16.8	4.0	6.9	0.19	5.6	608	207
2012	Séfa	V	x	x	x	x			x	x	x	x	x	x	x	x	x	x	x		x	x		23/07	F1/F2	49	12.5	2.8	4.8	0.16	5.5	653	120
2012	Sinthiou	C/V	x	x	x	x			x	x	x	x	x	x	x	x	x	x	x	x	x	x		17/07	F1/F2	52	10.2	3.3	5.7	0.17	5.6	363	251
2013	Darou	C/V	x			x	x	x		x	x	x		x		x	x	x	x	x	x	x	x	17/07	F1/F2	40	9.8	3.1	5.3	0.13	7.2	633	74
2013	Kolda	C									x	x				x		x						11/07	F1/F2	50	12.8	4.6	7.9	0.50	5.8	403	137
2013	Kolda	C/V	x			x	x	x		x	x	x		x		x	x	x	x	x	x	x	x	10/07	F1/F2	57	12.8	4.6	7.9	0.50	5.8	427	144
2013	Séfa	C/V									x	x				x		x						15/07	F1/F2	55	16.6	4.1	7.1	0.41	5.5	502	113
2013	Séfa	C/V	x			x	x	x		x	x	x	x	x	x	x	x	x	x	x	x			13/07	F1/F2	57	16.6	4.1	7.1	0.41	5.5	497	117
2013	Sinthiou	C/V	x			x	x	x		x	x	x		x		x	x	x	x	x	x	x	x	22/07	F1/F2	56	10.8	3.3	5.7	0.14	5.5	478	40
2013	Sinthiou	C									x	x				x		x						21/07	F1/F2	46	10.8	3.3	5.7	0.14	5.5	454	26
2013	Sinthiou	C									x	x				x		x						21/07	F1/F2	58	11.6	2.5	4.3	0.21	5.3	490	40
2014	Diéri Kao	V					x	x			x	x		x		x							x	02/8	F1/F2	20						382	79
2014	Kolda	C/V/P					x	x			x	x	x	x	x	x		x					x	03/8	F1/F2	60	16.8	4.0	6.9	0.19	5.6	553	38
2014	Kolda	C/V									x	x				x		x						02/8	F1/F2	58	16.8	4.0	6.9	0.19	5.6	540	51
2014	Ndama	V					x	x			x	x			x		x	x					x	11/8	F1/F2	26						350	42
2014	Sinthiou	C/V/P					x	x			x	x	x	x	x	x		x					x	24/07	F1/F2	56	11.5	3.1	5.3	0.30	5.7	382	85
2014	Sinthiou	C/V									x	x				x		x						08/8	F1/F2	54	11.2	2.8	4.9	0.16	5.5	347	30
2014	Sinthiou	C/V									x	x				x		x						25/07	F1/F2	49	13.9	3.0	5.1	0.36	5.7	414	53

Table 2 Characteristics of the cultivars used in the experiments in Senegal (identification, short name, name of the variety, genetical group, known cycle length in days to reach maturity and farmers use in Senegal). *n.a.* not available.

Identification	Short name	Variety	Genetical group	Cycle length (d)	Grown by farmers
1	DJ11	DJ11-509	Indica	100	Yes
2	DK17	Dkap 17	Hybrid	n.a.	No
3	DK2	Dkap 2	Hybrid	n.a.	No
4	DK3	Dkap 3	Hybrid	n.a.	No
5	FK45	FKR45N	Hybrid	95	No
6	INTA	Inta Fortaleza	Japonica	90–95	No
7	IR10	Irat 10	Indica	100	Yes
8	ITA	ITA 150	Japonica	100	Yes
9	NE1	Nerica 1	Hybrid	95–100	Yes
10	NE11	Nerica 11	Hybrid	75–85	No
11	NE12	Nerica 12	Hybrid	90–100	No
12	NE14	Nerica 14	Hybrid	75–85	No
13	NE17	Nerica 17	Hybrid	90–100	No
14	NE4	Nerica 4	Hybrid	95–100	No
15	NE6	Nerica 6	Hybrid	95–100	Yes
16	NE8	Nerica 8	Hybrid	75–85	No
17	NE9	Nerica 9	Hybrid	75–85	No
18	W181	Wab 181	Japonica	95	No
19	W189	Wab 189	Japonica	95	No
20	W5650	Wab 56-50	Japonica	100	Yes
21	WC165	Wab C165	Japonica	90	No

model is a process-based model that is embedded within DSSAT. It has been used to simulate rice growth and yield for decades (Buddhaboon et al. 2018). The climate driving variables have a daily time step: maximum and minimum air temperatures, solar radiation and precipitation, relative humidity, and wind speed when available. In DSSAT, potential evapotranspiration can be computed either using the Penman-Monteith equation following the method of Allen et al. (Allen et al. 1998) or using the Priestley and Taylor approach (Priestley and Taylor 1972). We used the more accurate Penman-Monteith approach in all the simulations using observed weather data, but used the Priestley-Taylor approach for simulations under future climate since CMIP5 models do not provide estimates of wind speed and relative humidity that are required for the Penman-Monteith approach. We used the global solar radiation as input data and applied a 0.5 ratio to get the photosynthetically active radiation. In DSSAT the soil is represented assuming horizontal homogeneity and considering a number of superposed horizontal soil layers. The soil properties of the 20–30 cm layer were applied to the below 30–100 cm horizon with a 50 % reduced C and N content. Soil water dynamics is simulated based on the classic reservoir analogy. Soil water retention parameters (soil moisture at wilting point and field capacity) are derived from soil texture (Gijsman et al. 2002). The crop model calculates a daily water stress factors as the ratio of soil water availability in the rooting zone over crop potential transpiration. Water stress reduces the rate of leaf growth, radiation conversion, and grain filling; accelerates senescence; and determines the ratio of actual over potential transpiration. Plant growth, development, and yield depend on species- and cultivar-dependent parameters determining the sensitivity of crops to variations in their environment. The rice team (i.e., a partnership between the International Fertilizer Development Center (IFDC), University of Florida, and the global Agricultural Model Intercomparison and Improvement Project (AgMIP)) has studied rice models under varying climatic conditions (Hasegawa et al. 2017) and proposed a new set of cultivar-dependent parameters, the so-called genetic coefficients, to ensure that CERES-Rice correctly simulated the effect of high temperatures, drought, and increases in atmospheric [CO_2]. These coefficients control crop development, such as flowering and maturing. There are eleven genetic coefficients defined in the CERES-Rice model. P1 (basic vegetative phase), P20 (critical photoperiod), and P2R (extent to which panicle initiation is delayed for each hour increase above P20) drive flowering onset. P5 is the length from flowering to grain maturity. G1 (potential spikelet number), G2 (single grain weight), G3 (relative tillering coefficient), and PHINT (phyllochron interval) influence crop growth and yield components. THOT, TCLDP, and TCLDS are the new temperature coefficients used to improve crop response to extreme temperatures. THOT drives spikelet sterility susceptibility to high temperatures; TCLDP and TCLDS modify respectively

panicle initiation and spikelet sterility when rice is exposed to low temperatures.

2.7 Model calibration and evaluation

The DSSAT model was calibrated and evaluated for the varieties evaluated in the trials (see Section 2.3). Calibration was done by combining a trial and error procedure with GENCALC calculator runs. GENCALC uses a deterministic stepwise procedure to optimize plant parameters within realistic physiological ranges (Buddhaboon et al. 2018). In a first step, we calibrated parameters related to crop phenology against observed flowering and maturity dates. P1, P20, and P2R were first adjusted so that simulated flowering date matched with the observed date. P5 was then adjusted to improve model agreement with observed maturity. In a second step, the tillering coefficient G3 was calibrated against observed aboveground biomass at flowering and harvest. Adjustment of G3 can alter plant phenology simulation; therefore, flowering-related parameters were re-adjusted. In the last step, G1, G2, and THOT were calibrated against observed yield and yield components. TCLDP and TCLDS remained unchanged in our calibration process.

The parameters were adjusted until there was a close match between observed and simulated values. Root mean square error (RMSE), EF, and d-stat index were used to evaluate model performance following the recommendations by Willmott (1982) for model evaluation, due to limitations in the use of the modeling efficiency (EF) as an agreement index.

$$RMSE = \sqrt{\frac{1}{n}\sum_{i=1}^{n}(y_i - x_i)^2}$$

$$EF = 1 - \frac{\sum_{i=1}^{n}(x_i - y_i)^2}{\sum_{i=1}^{n}(x_i - x_.)^2}$$

$$\text{d-stat} = 1 - \frac{\sum_{i=1}^{n}(y_i - x_i)^2}{\sum_{i=1}^{n}(|y_i - x_.| + |x_i - y_.|)^2}$$

where x_i is the i^{th} observed value, y_i the i^{th} simulated value, n the number of observations, $x_.$ the mean of the observed variable, and $y_.$ the mean of simulated variable.

These indicators for the calibration dataset are shown in Table 3. Flowering and maturity dates were fairly well simulated, i.e. observed and simulated mean values were similar, and RMSE was 3.2 and 3.9 days for flowering and maturity dates, respectively. Intermediate variables like aboveground biomass at anthesis and harvest, byproducts (straw), and harvest index were not very well simulated. Average simulated and observed values were similar, but RMSE was large. The number of grains was simulated with a RMSE of 1587, corresponding to 35% of the mean observed value. Measurement of aboveground biomass at anthesis and harvest required subplot sampling and transport. Drying usually occurred in suboptimal conditions, so that the estimates of aboveground biomass (dry matter) may not be as reliable as those for phenology, yield, and yield components that were obtained based on whole-plot sampling. Good correlation between observed and simulated grain yield were obtained in calibration (EF= 0.64, Supplementary materials: Fig 2a; d-stat = 0.9 and RMSE = 531) and validation (EF=0.47, Supplementary materials: Fig 2b; d-stat = 0.81 and RMSE = 405). Figure 2 shows the comparisons between simulated and observed values averaged for each cultivar, across years, fertilizer applications, and sites. Cultivar diversity with regard to number of panicles was not well reproduced by the model (EF = −1.26). Cultivar diversity with regard to number of grains, flowering date, and yield was adequately reproduced by the model with regression coefficients of 0.79, 0.90, and 0.77, respectively. We considered that the calibrated DSSAT model represented each cultivar with a good accuracy, especially for phenology, grain yield, and its components. Values of the genetic parameters used in CSM-CERES-Rice can be found in supplementary materials (Table S1).

2.8 Statistical analysis of the experiments

2.8.1 Tests on cultivars, years, and location effect and adjusted means

The set of tested cultivars varied across experiments (Table 1). For a fair comparison of cultivars, we adjusted their mean performance to account for year and location effects like in an incomplete block design. Conversely, we adjusted year and location effects to account for cultivar effect. We carried out F-tests of cultivar, year, and location effects using Kenward and Roger's method for the denominator degrees of freedom (Kenward and Roger 1997). The dataset used included all on-station controlled experiments conducted at the four sites during 3 years, with the two fertilizer rates and the 21 cultivars.

2.8.2 Detection of main varietal and environmental drivers of rice grain yield

In order to identify the key interactions between genotype traits and environments that were involved in yield variations, we conducted a covariance analysis on the dataset of on-station controlled experiment. The operational objective was to determine (i) the key features to be captured by the crop model and (ii) the key traits to account for when designing new ideotypes. We used the DSSAT genetic coefficients obtained from the calibration process as varietal covariates and soil and rainfall measurements in each trial as environmental covariates.

Table 3 Values of observed and simulated variables, number of observations, and statistical criteria used to assess the performance of the calibrated DSSAT model for rice in Senegal (EF, RMSE, d-Stat). EF model efficiency, RMSE root mean square error, d-Stat d-Stat index (see Willmott (1982))

Variable name	Mean		EF	RMSE	d-Stat.	Number of observations
	Observed	Simulated				
Anthesis (days)	66	66	0.53	3.24	0.826	182
Straw (kg ha $^{-1}$)	2029	2365	0.25	1415.5	0.671	182
Above ground biomass at anthesis (kg ha $^{-1}$)	3317	1705	0.12	2145.97	0.529	48
Above ground biomass at harvest (kg ha $^{-1}$)	3416	3728	0.41	1571.05	0.785	48
Grain number (nb m^{-2})	4519	4490	0.74	1587.8	0.917	182
Harvest index	0.34	0.33	0.19	0.148	0.659	48
Grain yield (kg ha $^{-1}$)	1187	1127	0.66	447.7	0.903	182
Seed weight g/unit	0.024	0.024	0.08	0.003	0.514	182
Maturity (days)	94	94	0.50	3.86	0.819	182
Panicles (nb m^{-2})	135.4	135.2	0.05	67.01	0.481	182

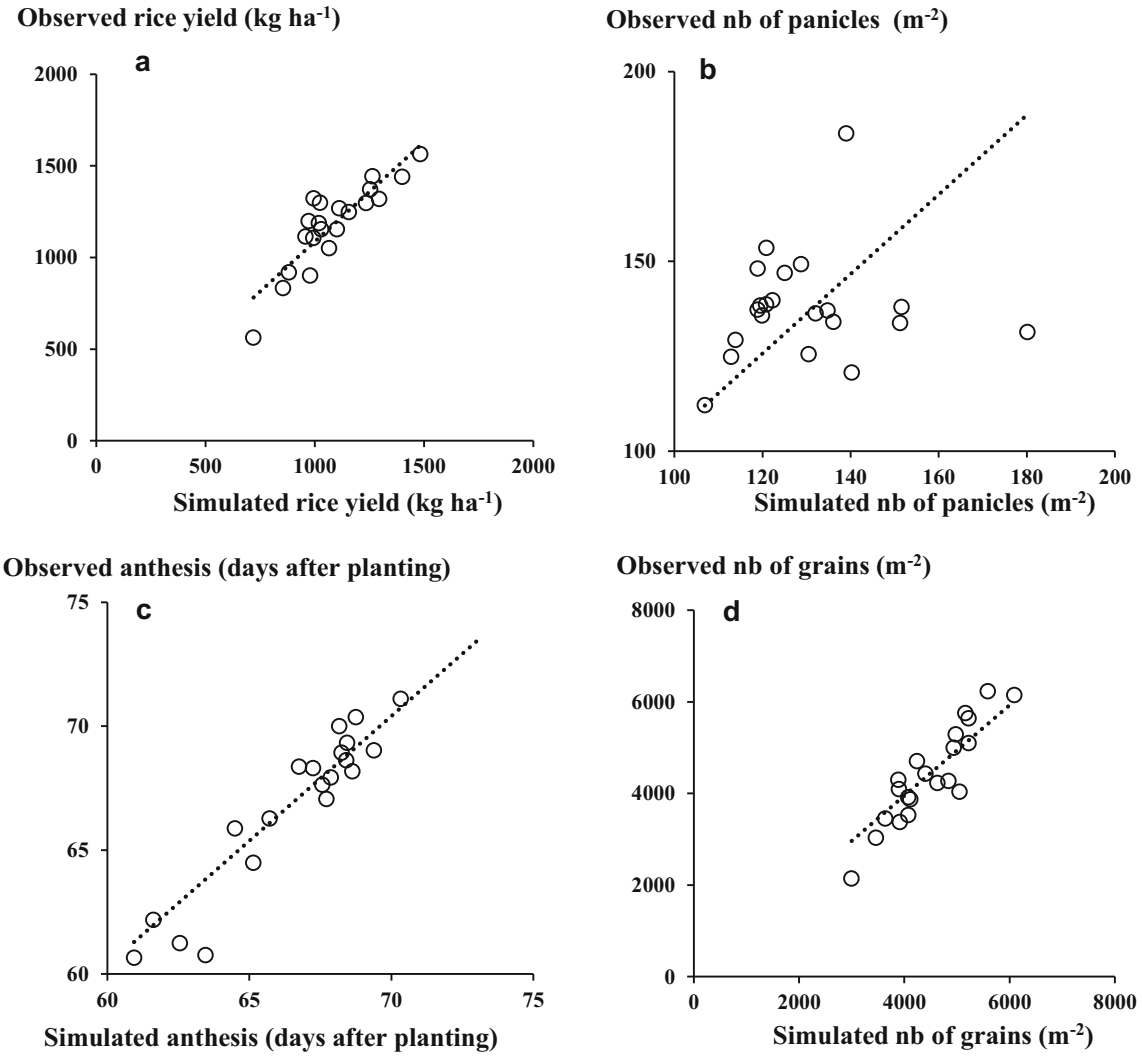

Fig. 2 Observed and simulated rice yield (a), number (nb) of panicles (b), number (nb) of grains (c) and anthesis day (d). Each dot is the average value for a given cultivar across years, fertilizer applications, and sites) Regression equations (dotted line): a: $y = 1.0865x$ with $r^2 = 0.766$; b: $y = 1.0475x$ with $r^2 = -1.266$; c: $y = 1.0058x$ with $r^2 = 0.8985$; d: $y = 0.9875x$ with $r^2 = 0.7936$.

The varietal covariates were P1, P2R, P5, P2O, G1, G2, G3, and THOT (supplementary materials, Table S1). The environmental covariates were sowing date, cumulated rainfall from sowing to 60 days after sowing (rain_0_60) and from 60 to 90 days after sowing (rain_60_90), soil nitrogen (N), carbon (C), and clay+silt content (Table 1).

In order to comply with the error structure of the multi-site design, we considered experiment, genotype, environment, and interactions as random effects for this analysis. The resulting full linear mixed model was:

$$Z_{ijkl} = m + \Sigma_p\, x_{pi}\, b_p + \Sigma_q\, y_{qj}\, c_q + A_i + B_j + (AB)_{ij} + c_k + (Ac)_{ik} + (Bc)_{jk} + (ABc)_{ijk} + D_{jl} + E_{ijkl}$$

where

Z_{ijkl}	is the observed yield for variety i with fertilization k in replicate l of environment j.
x_{1i}, x_{2i}... x_{Pi}	are the values of the P varietal covariates for variety i
y_{1j},y_{2j},... y_{Qj}	are the values of the Q environmental covariates for environment j
b_1...b_P	are the regression coefficients on varietal covariates
c_1...c_Q	are the regression coefficients on environmental covariates
A_i	is the random effect of variety i, remaining after the effects of its covariates
B_j	is the random effect of environment j, remaining after the effects of its covariates
$(AB)_{ij}$	is the random variety ×x environment interaction
c_k	is the fixed effect of fertilization level k
$(Ac)_{ik}$	is the random variety ×x fertilization interaction
$(Bc)_{jk}$	is the random environment ×x fertilization interaction
$(ABc)_{ijk}$	is the random variety ×x environment ×x fertilization interaction
D_{jl}	is the random effect of replicate l in environment j
E_{ijkl}	is the residual error

Due to its considerable range, grain yield had a residual variance increasing with its mean, thus suggesting a transformation in order to stabilize it: $(\text{grain yield})^{0.3}$ was analyzed rather than the original yield. Displayed means were back-transformed (Table 4).

In order to select which covariates should enter the model, we compared all models with or without each covariate with the Schwartz Bayesian information criterion (BIC). Best models have the smallest BICs, and we considered that models not differing by more than two BICs were equivalent. Among models for which BIC did not exceed the smallest BIC by more than two, we retained the model with the smallest number of covariates. Then, we checked the selected covariates for zero slope using a Student's t-test. We estimated the error degrees of freedom for this test with Kenward and Roger's method (Kenward and Roger 1997). We performed the mixed model analysis using SAS version 9.4.

2.9 Climate models

We used climate models projections of the Coupled Models Intercomparison Project (CMIP5) to generate the input weather data for DSSAT. These climate models simulations are widely used to estimate the effect of the increase in greenhouse gases emissions on climate. The results of climate model simulations are summarized in the IPCC report (AR5). Their resolutions range from 0.75° × 0.75° to 3.711° × 3.75° for rainfall and temperatures (Supplementary materials: Table S2).

We tested two climate change scenarios: RCP2.6 is representative of mitigation scenarios aiming at limiting the increase of global mean temperature to 2°C. RCP8.5 is representative of scenarios with high greenhouse gas emissions and absence of climate change policies. It leads to the greatest warming among scenarios, exceeding +4°C in some regions. Rainfall projections diverge substantially across models, especially for RCP8.5, for which models simulate either an increase or a decrease of rainfall in the future. Climate models do not accurately simulate the penetration of the rain belt during the monsoon season in West Africa (IPCC 2013). This can introduce biases when using the climate simulation with a crop model (Famien et al. 2018). To overcome this, Famien et al. (2018) used the cumulative distribution function transform method to correct GCMs outputs in order to mimic historical precipitation and temperatures with a resolution of 0.5° × 0.5° for each GCM. We applied this correction on future projections. Precipitation and temperatures simulated by seven climatic models and corrected by Famien et al. (2018) were used (Supplementary materials: Table S2). We choose seven models for their diversity based on the Monerie classification that groups models according to their simulated rainfall trend in the future (Monerie et al. 2017). Calibration of the climate models was done on years 1979 to 1996 and validation on years 1997–2013. This selection maximizes the spanned range of simulated rainfall for RCP2.6 and RCP8.5 scenarios for the twenty-first century and allows to explore better the possible climate change scenarios rather than using one median or average scenario.

Table 4 Anthesis date, maturity date, and rice yield means. Varietal means were adjusted for environment effects, and environment means were adjusted for varietal effects. Variety is sorted by anthesis date.

Factor	Level	Anthesis date (days)	Maturity date (day)	Rice yield (kg ha^{-1})
Variety	NE8	57.2	83.1	1115
	NE14	57.3	83.2	1313
	NE11	57.7	83.6	964
	NE9	58.0	83.9	906
	FK45	61.3	89.1	935
	INTA	63.3	91.2	1108
	ITA	63.6	91.4	700
	DK2	64.2	92.0	762
	NE17	64.5	92.3	862
	WC165	64.6	92.5	954
	W189	64.8	92.7	780
	DK3	65.2	93.2	605
	DJ11	65.7	93.6	981
	W5650	65.8	93.7	896
	W181	65.9	93.9	780
	NE1	66.2	94.1	568
	NE4	66.2	94.1	732
	NE12	67.6	95.4	525
	NE6	68.0	95.8	655
	DK17	68.2	96.1	351
	IR10	71.5	99.1	543
Fertilization	F1 (80 kg N ha^{-1})	63.7	91.2	1160
	F2 (20 kg N ha^{-1})	64.5	92.0	509
Site	Darou	64.0	91.3	269
	Kolda	64.8	92.4	1015
	Sinthiou Maleme	63.1	90.4	695
	Séfa	64.5	92.3	1589
Year	2012	64.1	91.6	1000
	2013	64.1	91.6	748
	2014	64.1	91.6	645

2.10 Ideotype construction

We used the cultivar coefficients of Nerica 8 (one of the best yielding cultivars in the experiments) as a starting point. We built 16 ideotypes by changing the values of four coefficients as follows: P1 +60 growing degree days, P5 +40 growing degree days, G1+30 spikelet per m^2, and THOT + 2°C. We explored all combinations of changed/unchanged coefficients resulting in $4^2 = 16$ virtual cultivars. We explored ideotypes performance in Sinthiou Maleme and Kolda, two contrasting sites representative of the range of environmental conditions found in Senegal for rainfed rice cultivation. Total rainfall at Sinthiou Maleme ranged 600 to 700 mm and soils were sandy (10 % clay + silt). Kolda had wetter conditions (900 to 1000 mm year^{-1}) and heavier soils (16.8 % clay + silt). For the simulations, plant population at seeding was set to 60 plants m^{-2} and row spacing to 0.6 m. Emergence dates were fixed on 8 July, and fertilization was set to 100 kg N ha^{-1} (applied at 1, 30, and 60 days after emergence). Independent simulations (i.e., the crop model was reset each year) were carried from 2000 to 2099 for each of the seven climate models. Simulated rice yields were then averaged across the seven climate models and across decades.

3 Results and discussion

3.1 Statistical analysis of the experiments

3.1.1 Tests of cultivar, year, and location effect and adjusted means

The adjusted cultivars, years, and location means for grain yield, anthesis, and maturity dates are shown in Table 4. Results of the tests for cultivar, year, and site effects are listed in Table 4. Cultivar yield varied widely, from 351 (DK17) to 1313 kg ha^{-1} (NE14). The best yielding cultivar (NE14) had the second shortest growth cycle: on average 57 and 83 days were required to reach anthesis and maturity, respectively. Cultivars with short cycle generally outperformed cultivars with longer cycles.

Fertilization greatly affected grain yield: cutting the recommended doses by 75% (from 80 to 20 kg N ha^{-1}) reduced the average grain yield by 651 kg ha^{-1}. There was a large yield differences between sites and years. Average yield at Darou was 17% of that at Sefa, and average yield dropped by 30% in 2013 and 2014 compared with 2012. By contrast, fertilization, site, and year had little or no effect on flowering and maturity dates. Only one significant genotype × environment interaction (between fertilization and year) was observed (Table 5).

Table 5 Covariance analysis of the rainfed rice cultivar experiments in Senegal from 2012 to 2014: test for the effect of fertilization, varietal, and environmental covariates. Denominator degrees of freedom (df) are computed following the method of Kenward and Roger (1997). G1, basic vegetative phase; THOT, spikelet sterility susceptibility to high.

Source	Numerator df	Denominator df	F-value	*p*-value
Fertilization	1	15.5	69.97	<.0001
G1	1	12.9	13.50	0.0029
THOT	1	15.5	6.08	0.0258
Sowing date	1	11.3	25.27	0.0004
Rain 0–60	1	10.6	6.31	0.0297
Soil N (‰)	1	10.6	5.47	0.0400
Soil C (‰)	1	10.7	6.39	0.0287
Clay + silt (%)	1	11.3	38.49	<.0001
Fertilization × year	2	7.0	5.15	0.0421

In 2012, a year with good rainfall, yield response to fertilization was greater than in the other years.

3.1.2 Genotypic and environmental drivers of grain yield variability

Using BIC criterion, the selected cultivar covariates were G1 and THOT. The selected environmental covariates were sowing date, rain 0–60 (cumulated rainfall from 0 to 60 days after sowing), soil N, soil C, and soil clay+silt. In the resulting model, all selected covariates had a significant effect (data not shown). Fertilization had the greatest F-value (Table 5) and was therefore the main controlled effect affecting yield, followed by soil clay+silt and sowing date. The selected covariates helped explain a substantial part of the varietal and environmental random variation: as compared to a model without covariates, the remaining varietal variance was reduced by 56% and the environmental variance by 89%. It means that the full model including the identified covariates captured half of the varietal effects and a large part of the environmental effect. The varietal covariates are included as genetic parameters in CSM-CERES-Rice; environmental covariates are the climate, soil, and crop management inputs of the model. For these reasons, the chosen crop model appears relevant to explore the performance of ideotypes.

The only significant interaction between treatment and environment was the fertilization × year interaction (Table 5). It can be explained by the fertilizer × rainfall interaction. Figure 3 shows the increase in observed and simulated rice yield (averaged per experiment across all cultivars) due to fertilizer (i.e., the difference between yield in F1, 80 kg N ha^{-1} and yield in F2, 20 kg N ha^{-1}). Variability due to cultivar (verticals error bars in Fig. 3) highlights the varietal diversity in response to fertilizer. The need for simultaneous and adequate supply of nitrogen and water is recognized worldwide especially in rainfed cereal cropping systems (Cossani et al. 2010). Water and nitrogen stresses interact to limit yields, so that the effect of the combined stress may be lower or greater than the effect of each stresses in isolation (Affholder 1995). For example, the benefits of adequate nitrogen supply for rice thanks to timely fertilizer application can be undermined if water stress occurs during vegetative phase. The large variability in yield response to nitrogen in the context of our study highlights a paradox: fertilizer application offers the promises of doubling rice yield (Table 4), but risk is high that a farmer will not get that yield increase if rainfall is not sufficient, especially at the end of the season after rice flowering. Therefore, policies targeting intensification strategies in such environment should include measures to mitigate those risks (e.g., insurance, weather forecast at different time horizon, crop diversification)

3.2 Climate data

A delay in monsoon onset and an increase in rainfall in the second period of the monsoon are expected by the end of the century (Biasutti 2013). With RCP8.5, the climate model MIROC-ESM-CHEM belonged to group 1 in Monerie's classification and simulated an increase in rainfall across the West African Sahel up to 20 °N and a moderate temperature increase. Group 3, the most populated group in CMIP5 exercise, includes models (HadGEM2-ES and IPSL-CM5A-LR) that predicted a decrease in rainfall in West Africa between 10 and 20°N, in relation with the strengthening of the inter-hemispheric SST gradient over the Atlantic with an enhancement of moisture flux convergence. Group 2 models (MPI-ESM-LR and MPI-ESM-MR) predicted a slight decrease in rainfall over West African Sahel without a relation with changes in moisture flux convergence but linked locally with changes in moisture recycling. On the other hand, group 4 models (e.g., bcc-csm1-1) depicted a decrease in rainfall across the same region (Monerie et al. 2017). Finally, NorESM1-M simulated an increase in rainfall (May to September).

Temperature projections in Sinthiou Maleme did not diverge substantially between climate models (Supplementary materials: Tables S3 and S4) as well as in Kolda (not shown). Confidence interval for Tmin and Tmax grew from 0.16 and 0.24 in 2000 to 0.21 and 0.57 in 2100, respectively. Projections are more consistent for Tmin than for Tmax, because Tmin is less impacted by cloud changes than Tmax. Climate models with RCP8.5 predicted an increase in Tmin and Tmax of 4.2 and 3.4 °C from 2000 to 2100, respectively. This greater increase in Tmin is related to a greater increase in temperature during the night than during the day, a common output of climate models (Lobell et al. 2007). Greater Tmin increases crop night respiration and lowers net photosynthesis. To account for this, crop models need a daily photosynthesis/respiration module. CSM-CERES-Rice does not have such

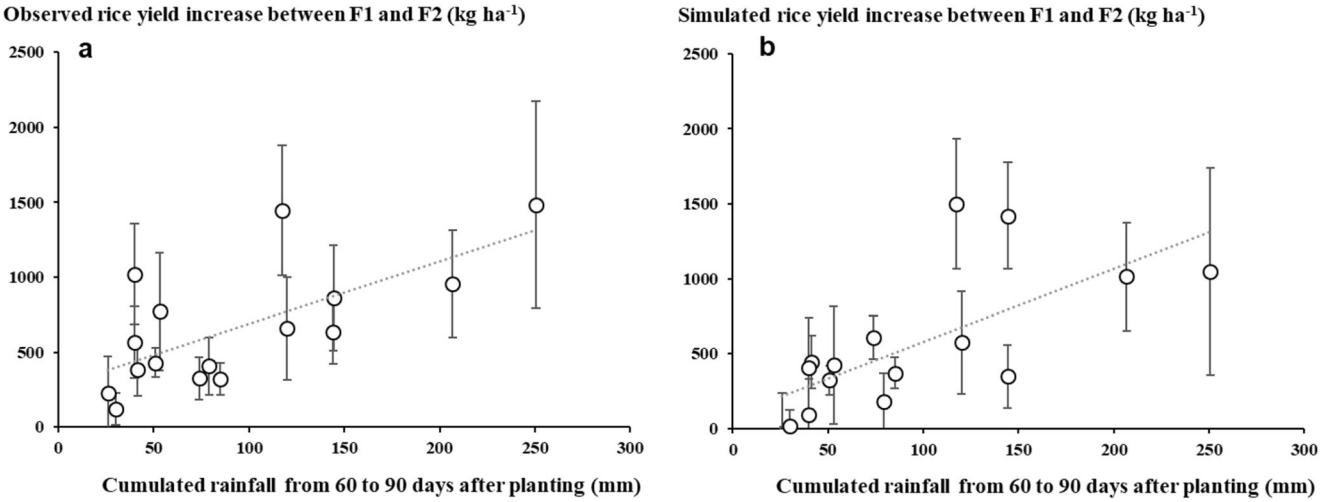

Fig. 3 Observed and simulated rice response to fertilization (difference between yield in F1, 80 kg N ha^{-1} and yield in F2, 20 kg N ha^{-1}) as a function of cumulated rainfall from 60 to 90 days after planting. Each dot is the mean difference for a given experiment, averaged across cultivars. Vertical bars are standard deviations. The dotted line is the regression of rice yield increase against cumulated rainfall. Observed yield (a): $y = 4.2x + 270$ with $r^2 = 0.46$ and simulated yield (b): $y = 4.9x + 89$ with $r^2 = 0.40$.

module. However, in the latest version, the new cultivar parameter THOT allows to account for heat effect on spikelet sterility, number of grains, and grain yield. There was no clear trend over the century in the global solar radiation. All models predicted more or less 20 MJ m^2 day^{-1} (see Supplementary materials Table S5).

Models diverged with regard to rainfall simulations. For example, ME simulated an increase in annual rainfall over the century with RCP8.5 (Table 6), while the 6 other climate models simulated a decrease. This highlights the need to use an ensemble of climate models to study climate change impacts. Table 6 shows the simulated average decadal rainfall and its confidence interval for the seven climate models from 2000 to 2100 in Sinthiou Maleme. Temperature in the other locations followed similar trends (data not shown). Simulated average daily rainfall from May to November declined at a rate of 0.05 mm $year^{-1}$. Over 100 years, total rainfall decreased by 50 mm ± 100 mm on average at that site (Table 6). However, the confidence interval was larger than the expected decrease. This decrease in rainfall will likely cause an increase in drought stress if farmers intensify rice production with more balanced and appropriate nutrient applications. The simulated average decrease in total rainfall hides intra-season differences. The main simulated drop occurred in August: average daily rainfall in this month decreased by 3.9 mm $year^{-1}$ (data not shown). No reduction in average daily rainfall was expected in October and a very limited one in June (0.5 mm per year, data not shown). Thus, rice sowing date will remain unchanged, and the expected length of growing season from June to October will be similar, but heavy rains in August will be less frequent. Consequently, on one hand, the crop might have enough time to mature before the end of the rainy season. On the other hand, warming will accelerate crop development. Accordingly, no direct link can be drawn "a priori" between a reduction of rainfall amounts and a reduction of yield without the use of a model to simulate soil/climate/management interactions on plant growth, water, and nitrogen availability.

3.3 Crop yields simulations

3.3.1 Global trends in rice yields

Figure 4 shows the trends in the decadal average of simulated rice yield with recommended fertilization (80 kg N ha^{-1}) and Nerica 8 for the seven climatic models, with and without the effect of elevated [CO_2], for RCP2.6 and 8.5, in Sinthiou Maleme. With RCP2.6 and consideration of CO_2 effect, rice yield will increase from 3600 in 2000–2009 to 4500 kg ha^{-1} in 2090–2099 (Fig. 4a). For all climate model projections (except IL and MM), the crop model predicted an increase in yield.

This "fertilizing" effect of CO_2 is well known, especially for C3 crops. Though it used to be controversial, it is now supported by recent findings from multiple free-air CO2 enrichment (FACE) experiments on soybean, rice, cotton, and wheat (Long et al. 2006). The future increases in crop production caused by the aerial fertilization effect of the atmosphere's rising [CO_2] may well be *twice* as large as what FACE experiments suggest (Bunce 2013). A recent review showed that the effect of elevated [CO_2] on C3 crops (Makowski et al. 2020) with adaptation practices can offset the yield decline due to temperature increase (estimated to be 2.4% yield decrease per °C increase in temperature), even at +4 °C. However, this positive effect cannot offset yield decline caused by temperature increase above 4°C (Xiong et al. 2007). Without the effect of elevated [CO_2]

Table 6 Decadal average of seasonal rainfall (mm day^{-1}) for two RCPs and seven climatic models in Sinthiou Maleme. *RCP* Representative Concentration Pathways; climate models: *BC* bcc-csm1-1, *HE* HadGEM2-ES, *IL* IPSL-CM5A-LR, *ME* MIROC-ESM-CHEM, *ML* MPI-ESM-LR, *MM* MPI-ESM-MR, *NM* NorESM1-M. More details on climate models are given in SI Table S2

		2000–2009	2010–2019	2020–2029	2030–2039	2040–2049	2050–2059	2060–2069	2070–2079	2080–2089	2090–2099
RCP 2.6	Mean	3.10	3.02	3.01	3.12	3.18	3.09	3.18	3.34	3.12	3.31
	Confidence interval	0.27	0.31	0.39	0.37	0.49	0.50	0.59	0.50	0.53	0.62
	BC	2.89	3.52	3.85	3.37	3.38	3.39	3.60	3.52	3.23	3.17
	HE	3.27	3.21	2.66	2.61	3.47	2.92	2.95	3.92	3.13	3.40
	IL	3.19	2.87	2.76	2.45	2.26	2.45	2.39	2.52	2.19	2.50
	ME	3.53	3.41	3.49	3.66	4.26	4.49	4.88	4.28	4.52	4.99
	ML	3.14	2.31	2.39	3.15	2.60	2.45	2.63	2.77	2.60	2.82
	MM	2.60	2.45	2.35	2.83	2.37	2.35	2.26	2.34	2.33	2.14
	NM	2.57	3.09	3.11	2.87	3.43	3.20	3.40	3.40	3.67	3.41
RCP 8.5	Mean	2.97	2.80	2.83	2.99	2.83	2.73	2.74	2.68	2.55	2.44
	Confidence interval	0.20	0.29	0.36	0.43	0.54	0.68	0.89	0.94	1.06	1.18
	BC	3.38	3.10	3.20	3.24	2.73	3.07	3.03	2.86	2.75	2.59
	HE	2.96	2.56	2.49	2.78	2.51	1.91	1.78	1.80	1.32	1.07
	IL	2.49	2.39	2.18	2.32	2.17	1.97	1.50	1.94	1.42	1.16
	ME	3.18	3.05	3.78	4.00	4.34	4.69	5.12	5.31	5.08	5.29
	ML	2.94	2.34	2.49	2.32	2.81	2.08	1.89	1.60	1.32	1.21
	MM	2.72	2.64	2.45	2.69	1.96	1.86	1.78	1.64	1.66	1.15
	NM	3.19	2.75	2.95	2.89	2.55	2.87	2.79	2.17	2.14	2.28

(Fig. 4b), simulated rice yield stagnated over the century. Figure 4c and d show trends in decadal average of simulated rice yield for the pessimistic RCP8.5 scenario. This scenario could be realistic given the lack of mitigation effort put in place by the industrial countries driving global emissions. Assuming no adaptation, average simulated rice yield will be divided by two by the end of the century. However, simulated yields differed strongly across climate models. With ME and BC climate models, the crop model simulated an increase in yield from 2700–2800 in 2000s to 3200–3500 kg ha^{-1}in the 2050s, while it predicted a large decrease (below 2000 kg ha^{-1}) with the other climate models. ME and BC simulated more rainfall than the other models (Table 6). ME predicted an increase in average daily rainfall from 3 to 5 mm by the end of the century (Table 6), as a consequence the crop model simulated an increase in rice yield.

3.3.2 Designing ideotypes

Since crop model simulations with all GCMs predicted a decrease in rice yield in Sinthiou Maleme with RCP8.5 (Fig. 4c and d), breeding for new cultivars that are tolerant and adapted to higher temperatures can contribute to adaptation of cropping systems. This increase in temperature causes a shortening of rice phenological stages in days. The rainy season will probably have an unchanged start and duration. Relevant adaptation traits include an increase in the thermal time (degree days) to reach flowering or grain filling to regain this loss in crop cycle duration. Higher tolerance to extreme temperature would also help reduce the negative impacts of days with extreme temperature. Higher productivity would also be positive if possible to achieve. Table 7 shows the simulated relative yield increase with 15 ideotypes derived from Nerica 8 for all GCMs with RCP8.5, in Sinthiou Maleme and Kolda. It shows large differences in yield advantage according to ideotypes. In the baseline periods (2000 to 2020, Table 7), a cultivar with a longer vegetative phase (increase in P1) would produce 13–17% more than Nerica 8 in Kolda, and a cultivar with more spikelets or a better tolerance to high temperature (increase in G1 or THOT) would produce 16 % more than Nerica 8 in Sinthiou Maleme. For mid and long term, interactions between ideotypes and future climate are similar in both sites. However, potential increase in yield with the ideotypes with all parameters changed was greater in

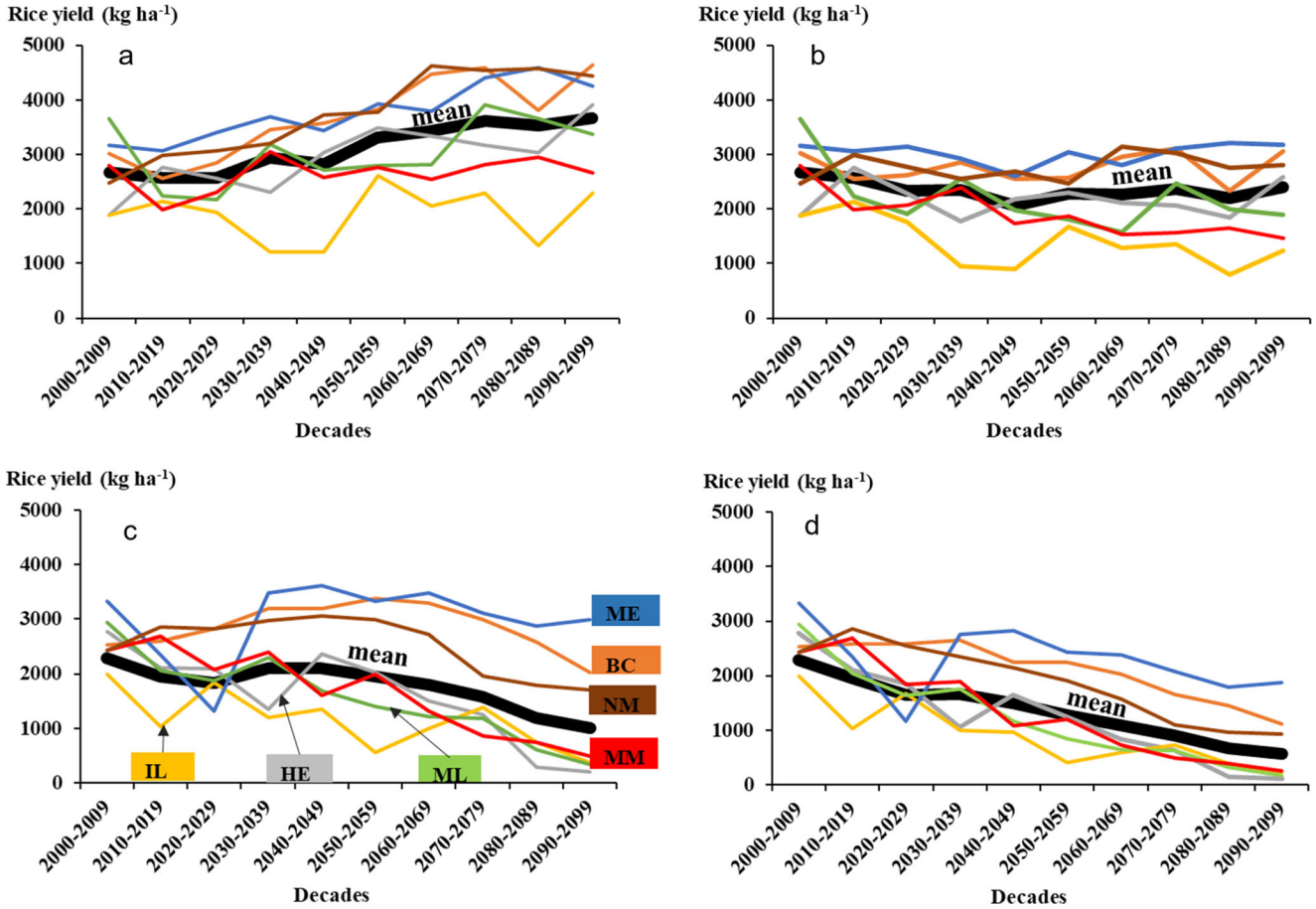

Fig. 4 Decadal average of simulated rice yield in Sinthiou Maleme over the century for two RCP (Representative Concentration Pathways), seven climate models. a: RCP 2.6 with CO_2 fertilizing effect, b: : RCP 2.6 without CO_2 fertilizing effect, c: RCP 8.5 with fertilizing CO_2 effect, d: RCP 8.5 without CO_2 fertilizing effect. For the abbrevations of the climate models please see supplementary materials Table S2.

Kolda (32% in 2090–2100) than in Sinthiou Maleme (10% in 2090–2100). Cultivars with longer vegetative phase (increase in P1) were more productive than their unmodified counterparts. On the contrary, ideotypes with increased time for grain filling were less productive than their counterparts without changes. By the end of the century, ideotypes with longer time for grain filling (n° 5, 7, 14, and 15) will be more productive. Some ideotypes performed better than Nerica8 at the beginning of the century (e.g., n°1 in Kolda), but this yield advantage decreased over time as climate change became more prominent. Conversely, the two ideotypes with increase in P5, G1, and THOT (n°14 and 15) had lower yield advantage with current climate and greater yield advantage at the end of the century (2050 to 2100), where simulated temperatures were greater. The best ideotype (n°7) had changes in P1, G1, and THOT coefficients: it had a yield advantage and stability in the two locations, regardless of the time period considered.

Cultivars with changes in P5 (grain filling duration) and G1 (number of spikelets) need more time to reach maturity and produce more spikelets. They belong to the new plant type (NPT) obtained through crosses with japonica types. They have a high sink capacity often not met by carbohydrates offer. Their simulated yield advantage during the first half of the century was negative (see Table 7, n°12, 13, 14, and 15). Interestingly, after 2050, as carbon supply by the atmosphere increased, their yield advantage became positive if THOT was also increased (n°14 and 15). This interaction between sink strength and source limitations was simulated on irrigated rice by Aggarwal et al. (1997). Our results are also in line with a recent evolutionary analysis over 20,000 years, which concluded that breeding programs and ideotypes construction needed to focus on sink strength capacity (Dingkuhn et al. 2020). Breeders need different genetic engineering toolboxes for the creation of ideotypes with different source-sink and assimilate partitioning. The principle is to match simultaneously photosynthesis carbon offer to a growing demand. For example, modifying T6P genes expression, the regulators of photosynthesis downregulation, and targeting the size and the number of organs were demonstrated to be a promising strategy for maize breeders (Nuccio et al. 2015).

To summarize, we predicted a sharp decline in rainfed rice yield in Senegal under climate change along the twenty-first

Table 7 Average relative change (%) in simulated decadal rice yield for 15 ideotypes compared with Nerica 8. Scenario RCP 8.5 and projection of 7 GCMs at two sites (Kolda and Sinthiou Maleme) were considered. The coefficient identified in the Black box were modified from Nerica 8 as follows: P1, P1 +60 growing degree days; P5, P5 +40 growing degree days; G1, G1+30 spikelets per m^2, THOT: Thot + 2°C). RCP, Representative Concentration Pathways; GCM, Global Climate Models; P1, basic vegetative phase; P5, length from flowering to grain maturity; THOT, drives spikelet sterility susceptibility to high temperatures. Color codes: red = very negative (relative change < –9); light red = negative (–10 < relative change < 0) ; white = no changes (6 > relative change >–5) ; light blue = positive (11 > relative change > 5) ; blue = very positive (relative change > 10).

					Kolda										Sinthiou Maleme									
N°	P1	P5	G1	Thot	2000 2009	2010 2019	2020 2029	2030 2039	2040 2049	2050 2059	2060 2069	2070 2079	2080 2089	2090 2099	2000 2009	2010 2019	2020 2029	2030 2039	2040 2049	2050 2059	2060 2069	2070 2079	2080 2089	2090 2099
1	■				17	16	13	10	9	7	6	3	5	-1.0	9	7	9	7	7	4.8	-5	-12	-16	-22
2				■	0	-1	-1	-1	0	0	0	0	0	-0	0	0	0	0	0	0	0	0.7	1	1
3	■			■	6	7	8	8	11	12	13	12	13	13	9	10	9	11	14	15	17	18	20	21
4			■		4	5	5	5	5	5	6	6	6	6	6	7	6	6	7	6.9	7	7	8.6	8
5	■		■		10	12	13	13	16	17	18	17	18	18	16	16	15	17	21	22	23	25	28	29
6			■	■	3	5	4	4	5	6	6	6	6	6	7	7	6	7	8	7	8	8	9	9
7	■		■	■	9	12	12	12	15	16	18	17	18	18	16	16	15	17	21	22	24	25	29	29
8		■			-26	-25	-24	-21	-19	-17	-15	-14	-14	-14	-25	-23	-21	-18	-16	-17	-16	-15	-16	-15
9	■	■			-20	-19	-17	-15	-10	-8	-5	-3	-3	-4	-18	-16	-14	-9	-5	-5	-2	0	0	3
10		■		■	-26	-25	-24	-21	-19	-17	-15	-14	-14	-14	-25	-23	-21	-18	-16	-17	-16	-14	-16	-14
11	■	■		■	-20	-19	-17	-15	-10	-8	-5	-4	-3	-4	-18	-16	-15	-9	-5	-5	-3	0	1	3
12		■	■		-22	-21	-19	-17	-14	-12	-10	-9	-9	-10	-20	-18	-16	-12	-10	-12	-10	-8	-9	-8
13	■	■	■		-17	-15	-14	-11	-6	-3	0	1	1	0	-13	-10	-9	-4	1	0	3	6	7	9.7
14		■	■	■	-25	-22	-20	-11	-10	-1	6	10	17	23	-20	-17	-16	-12	-10	-11	-10	-7	-8	-7
15	■	■	■	■	-21	-17	-13	-6	-2.4	7	15	18	27	33	-13	-11	-9	-4	1	0	4	7	8	10

century if no climate mitigation and no cropping adaptation occurs. We also showed that, given the range of genetic variability we had in our hand, breeding for new cultivar is possible to get more resilient cultivars. Ideotypes with a longer vegetative phase and a higher sink demand to match the increase in carbon supply by the atmosphere offer a real potential for high yielding and resilient cultivars. To our knowledge, this is the first time that a study using a process-based crop model coupled with an ensemble of global circulation models quantifies the rice yield trends in West Africa under climate change and thoroughly identifies ideotypes to set priorities for breeding programs.

4 Conclusions

In this study, the potential impacts of climate change on rainfed rice yield were assessed for RCP2.6 and 8.5 at different sites representative of a rainfall gradient in Senegal. Our study based on crop model simulations with future climate identified promising ideotypes that can help set priorities for rainfed rice breeding in the region. Farmers currently grow long cycle cultivars, while hybrids with shorter cycles associated with high fertilization rates could yield more with current climate. Climate models predict a decrease in rainfall and an increase in temperature in the future that cause a decline in simulated rice yield if no adaptation occurs. We showed that new cultivars with longer vegetative phase could partially offset the simulated yield losses. Better tolerance to high temperatures and higher sink capacity with increased number of tillers and spikelets also conferred yield advantage over the current best-performing cultivar. This is the first time that adaptive traits and ideotypes of rainfed rice adapted to current and future conditions in West Africa are defined in such physiological terms using up-to-date climatic predictions.

Supplementary Information The online version contains supplementary material available at https://doi.org/10.1007/s13593-021-00710-2.

Authors' contributions Conceptualization, E.Gé., B.S., and F.A.; methodology, E.Gé., D.D., B.S., and B.M.; investigation, P.M.K. and B.M.; formal analysis, D.D., B.S., E.Gé., and E.Go.; writing (original draft), E.Gé.; writing (review and editing), E.Gé., G.F., B.S., F.A., E.Go., and R.L.; funding Acquisition, B.M. and B.S.

Funding This study was funded by AfricaRice-CCAFS for the experiments and AMMA 2050 (NERC/DFID, grant number NE/M020126/1) for the climatic predictions.

Data availability The datasets analyzed during the current study are available from the corresponding author on reasonable request.

Declarations

Ethics approval not applicable

Conflict of interest The authors declare no competing interests.

References

Affholder F (1995) Effect of organic matter input on the water balance and yield of millet under tropical dryland condition. Field Crop Res 41:109–121. https://doi.org/10.1016/0378-4290(94)00115-S

Aggarwal PK, Kropff MJ, Cassman KG, ten Berge HFM (1997) Simulating genotypic strategies for increasing rice yield potential in irrigated, tropical environments. Field Crop Res 51:5–17. https://doi.org/10.1016/S0378-4290(96)01044-1

Allen RG, Pereira LS, Raes D, Smith M (1998) Crop evapotranspiration —guidelines for computing crop water requirements. FAO Irrigation and drainage paper 56. Food and Agriculture Organization, Rome. http://www.fao.org/docrep/x0490e/x0490e00.htm

Barry AA, Caesar J, Klein Tank AMG, Aguilar E, McSweeney C, Cyrille AM, Nikiema MP, Narcisse KB, Sima F, Stafford G, Touray LM, Ayilari-Naa JA, Mendes CL, Tounkara M, Gar-Glahn EVS, Coulibaly MS, Dieh MF, Mouhaimouni M, Oyegade JA, Sambou E, Laogbessi ET (2018) West Africa climate extremes and climate change indices. Int J Climatol 38:e921–e938. https://doi.org/10.1002/joc.5420

Biasutti M (2013) Forced Sahel rainfall trends in the CMIP5 archive. J Geophys Res-Atmos 118:1613–1623. https://doi.org/10.1002/jgrd.50206

Boote KJ, Jones JW, Batchelor WD, Nafziger ED, Myers O (2003) Genetic coefficients in the CROPGRO-soybean model: links to field performance and genomics. Agron J 95:32–113. https://doi.org/10.2134/agronj2003.3200

Buddhaboon C, Jintrawet A, Hoogenboom G (2018) Methodology to estimate rice genetic coefficients for the CSM-CERES-Rice model using GENCALC and GLUE genetic coefficient estimators. J Agric Sci 156:482–492. https://doi.org/10.1017/S0021859618000527

Bunce JA (2013) Effects of pulses of elevated carbon dioxide concentration on stomatal conductance and photosynthesis in wheat and rice. Physiol Plant 149:214–221. https://doi.org/10.1111/ppl.12026

Cossani CM, Slafer GA, Savin R (2010) Co-limitation of nitrogen and water, and yield and resource-use efficiencies of wheat and barley. Crop Past Sci 61:844–851. https://doi.org/10.1071/CP10018

Diedhiou A, Bichet A, Wartenburger R, Seneviratne SI, Rowell DP, Sylla MB, Diallo I, Todzo S, Touré NE, Camara M, Ngatchah BN, Kane NA, Tall L, Affholder F (2018) Changes in climate extremes over West and Central Africa at 1.5 °C and 2 °C global warming. Environ Res Lett 13:065020. https://doi.org/10.1088/1748-9326/aac3e5

Dingkuhn M, Luquet D, Fabre D, Muller B, Yin X, Paul MJ (2020) The case for improving crop carbon sink strength or plasticity for a CO2-rich future. Curr Opin Plant Biol 56:259–272. https://doi.org/10.1016/j.pbi.2020.05.012

Famien AM, Janicot S, Ochou AD, Vrac M, Defrance D, Sultan B, Noël T (2018) A bias-corrected CMIP5 dataset for Africa using the CDF-t method – a contribution to agricultural impact studies. Earth Syst Dyn 9:313–338. https://doi.org/10.5194/esd-9-313-2018

Gijsman AJ, Jagtap SS, Jones JW (2002) Wading through a swamp of complete confusion: how to choose a method for estimating soil water retention parameters for crop models. Eur J Agron 18:77–106. https://doi.org/10.1016/S1161-0301(02)00098-9

Glatzel K (2018) What can we learn from rising rice production in Senegal?, IFPRI, Dakar, Senegal, pp. Issue Post. https://www.ifpri.org/blog/what-can-we-learn-rising-rice-production-senegal. Accessed 29 June 2021

Hasegawa T, Li T, Yin X, Zhu Y, Boote K, Baker J, Bregaglio S, Buis S, Confalonieri R, Fugice J, Fumoto T, Gaydon D, Kumar SN, Lafarge T, Marcaida Iii M, Masutomi Y, Nakagawa H, Oriol P, Ruget F, Singh U, Tang L, Tao F, Wakatsuki H, Wallach D, Wang Y, Wilson LT, Yang L, Yang Y, Yoshida H, Zhang Z, Zhu J (2017) Causes of variation among rice models in yield response to CO2 examined with free-air CO2 enrichment and growth chamber experiments. Sci Rep 7:14858. https://doi.org/10.1038/s41598-017-13582-y

IPCC (2013) In: Stocker TF, Qin D, Plattner G-K, Tignor M, Allen SK, Boschung J, Nauels A, Xia Y, Bex V, Midgley PM (eds) Climate Change 2013: The Physical Science Basis. Contribution of Working Group I to the Fifth Assessment Report of the Intergovernmental Panel on Climate Change. IPCC, Cambridge and New York, p 1535

Jagadish SVK, Murty MVR, Quick WP (2015) Rice responses to rising temperatures – challenges, perspectives and future directions. Plant Cell Environ 38:1686–1698. https://doi.org/10.1111/pce.12430

Jayne TS, Mason NM, Burke WJ, Ariga J (2018) Review: taking stock of Africa's second-generation agricultural input subsidy programs. Food Policy 75:1–14. https://doi.org/10.1016/j.foodpol.2018.01.003

Kenward MG, Roger JH (1997) Small sample inference for fixed effects from restricted maximum likelihood. Biometrics 53:983–997. https://doi.org/10.2307/2533558

Kontgis C, Schneider A, Ozdogan M, Kucharik C, Tri VPD, Duc NH, Schatz J (2019) Climate change impacts on rice productivity in the Mekong River Delta. Appl Geogr 102:71–83. https://doi.org/10.1016/j.apgeog.2018.12.004

Koudahe K, Djaman K, Bodian A, Irmak S, Sall M, Diop L, Balde AB, Rudnick DR (2017) Trend analysis in rainfall, reference evapotranspiration and aridity index in southern Senegal: adaptation to the vulnerability of rainfed rice cultivation to climate change. Atmos Clim Sci 07(04):20–495. https://doi.org/10.4236/acs.2017.74035

Li T, Hasegawa T, Yin X, Zhu Y, Boote K, Adam M, Bregaglio S, Buis S, Confalonieri R, Fumoto T, Gaydon D, Marcaida M III, Nakagawa H, Oriol P, Ruane AC, Ruget F, Singh B, Singh U, Tang L, Tao F, Wilkens P, Yoshida H, Zhang Z, Bouman B (2015) Uncertainties in predicting rice yield by current crop models under a wide range of climatic conditions. Glob Chang Biol 21:1328–1341. https://doi.org/10.1111/gcb.12758

Lobell D, Bonfils C, Duffy P (2007) Climate change uncertainty for daily minimum and maximum temperatures: a model inter-comparison. Geophys Res Lett 34. https://doi.org/10.1029/2006GL028726

Long SP, Ainsworth EA, Leakey AD, Nösberger J, Ort DR (2006) Food for thought: lower-than-expected crop yield stimulation with rising CO2 concentrations. Science 312:1918–1921. https://doi.org/10.1126/science.1114722

Makowski D, Marajo-Petitzon E, Durand J-L, Ben-Ari T (2020) Quantitative synthesis of temperature, CO2, rainfall, and adaptation effects on global crop yields. Eur J Agron 115:126041. https://doi.org/10.1016/j.eja.2020.126041

Monerie P-A, Sanchez-Gomez E, Boé J (2017) On the range of future Sahel precipitation projections and the selection of a sub-sample of CMIP5 models for impact studies. Clim Dyn 48(7-8):2751–2770. https://doi.org/10.1007/s00382-016-3236-y

Nuccio ML, Wu J, Mowers R, Zhou H-P, Meghji M, Primavesi LF, Paul MJ, Chen X, Gao Y, Haque E, Basu SS, Lagrimini LM (2015) Expression of trehalose-6-phosphate phosphatase in maize ears improves yield in well-watered and drought conditions. Nat Biotechnol 33:862–869. https://doi.org/10.1038/nbt.3277

Oort P, Zwart S (2017) Impacts of climate change on rice production in Africa and causes of simulated yield changes. Glob Chang Biol 24:24–1045. https://doi.org/10.1111/gcb.13967

Priestley CHB, Taylor RJ (1972) On the assessment of surface heat flux and evaporation using large-scale parameters. Mon Weather Rev 100:81–92. https://doi.org/10.1175/1520-0493(1972)100%3C0081:OTAOSH%3E2.3.CO;2

Rötter RP, Tao F, Höhn JG, Palosuo T (2015) Use of crop simulation modelling to aid ideotype design of future cereal cultivars. J Exp Bot 66:3463–3476. https://doi.org/10.1093/jxb/erv098

Roudier P, Sultan B, Quirion P, Berg A (2011) The impact of future climate change on West African crop yields: what does the recent literature say? Glob Environ Change 21:1073–1083. https://doi.org/10.1016/j.gloenvcha.2011.04.007

Sheehy JE, Dionora MJA, Mitchell PL (2001) Spikelet numbers, sink size and potential yield in rice. Field Crop Res 71:77–85. https://doi.org/10.1016/S0378-4290(01)00145-9

Traore S, Zhang L, Guven A, Fipps G (2020) Rice yield response forecasting tool (YIELDCAST) for supporting climate change adaptation decision in Sahel. Agric Water Manag 239:106242. https://doi.org/10.1016/j.agwat.2020.106242

Willmott CJ (1982) Some comments on the evaluation of model performance. Bull Am Meteorol Soc 63:1309–1313. https://doi.org/10.1175/1520-0477(1982)063<1309:SCOTEO>2.0.CO;2

Xiong W, Lin E, Ju H, Xu Y (2007) Climate change and critical thresholds in China's food security. Clim Chang 81:205–221. https://doi.org/10.1007/s10584-006-9123-5

Yao F, Xu Y, Lin E, Yokozawa M, Zhang J (2007) Assessing the impacts of climate change on rice yields in the main rice areas of China. Clim Chang 80:395–409. https://doi.org/10.1007/s10584-006-9122-6

Zhang L, Traore S, Ge J, Li Y, Wang S, Zhu G, Cui Y, Fipps G (2019) Using boosted tree regression and artificial neural networks to forecast upland rice yield under climate change in Sahel. Comput Electron Agric 166:105031. https://doi.org/10.1016/j.compag.2019.105031